molecules. However, the effects for immune responses induced by other neoglycolipids have not been studied at all so far. We have a great interest in this issue and are seeking the materials with immunoregulatory properties. If such materials would be found, our neoglycolipid-coated liposome technology might be further applicable for antigen-specific regulation of autoimmune diseases and allergy.

Acknowledgement

This work was supported by the Industrial Technology Research Grant Program of the New Energy and Industrial Technology Development Organization (NEDO) of Japan, in part by a grant for Hi-tech research program from Tokai University, and by the Program for Promotion of Basic Research Activities for Innovative Biosciences (PROBRAIN).

References

1. Gattinoni L, Powell DJ Jr, Rosenberg SA, Restifo NP. 2006. Adoptive immunotherapy for cancer: building on success. *Nat. Rev. Immunol.* 6: 383-393.
2. Rosenberg SA, Yang JC, Restifo NP. 2004. Cancer immunotherapy: moving beyond current vaccines. *Nat. Med.* 10: 909-915.
3. Rosenberg SA. 2001. Progress in the development of immunotherapy for the treatment of patients with cancer. *J. Intern. Med.* 250: 462-475.
4. Boon T, Coulie PG, Van den Eynde BJ, van der Bruggen P. 2006. Human T cell responses against melanoma. *Annu. Rev. Immunol.* 24: 175-208.
5. Pardoll DM, Topalian SL. 1998. The role of $CD4^+$ T cell responses in antitumor immunity. *Curr. Opin. Immunol.* 10: 588-594.
6. Wang RF, Peng G, Wang HY. 2006. Regulatory T cells and Toll-like receptors in tumor immunity. *Semin. Immunol.* 18: 136-142.
7. Sakaguchi S, Setoguchi R, Yagi H, Nomura T. 2006. Naturally arising Foxp3-expressing $CD25^+CD4^+$ regulatory T cells in self-tolerance and autoimmune disease. *Curr. Top. Microbiol. Immunol.* 305: 51-66.
8. Leen AM, Rooney CM, Foster AE. 2007. Improving T cell therapy for cancer. *Annu. Rev. Immunol.* 25: 243-265.
9. Ikehara Y, Kojima N. 2007. Development of a novel oligomannose-coated liposome-based anticancer drug-delivery system for intraperitoneal cancer. *Curr. Opin. Mol. Ther.* 9: 53-61.
10. Ikehara Y, Niwa T, Biao L, Ikehara SK, Ohashi N, Kobayashi T, Shimizu Y, Kojima N, Nakanishi H. 2006. A carbohydrate recognition-based drug delivery and controlled release system using intraperitoneal macrophages as a cellular vehicle. *Cancer Res.* 66: 8740-8748.
11. Krist LF, Kerremans M, Broekhuis-Fluitsma DM, Eestermans IL, Meyer S, Beelen RH. 1998. Milky spots in the greater omentum are predominant sites of local tumour cell proliferation and accumulation in the peritoneal cavity. *Cancer Immunol. Immunother.* 47: 205-212.
12. Hagiwara A, Takahashi T, Sawai K, Taniguchi H, Shimotsuma M, Okano S, Sakakura C, Tsujimoto H, Osaki K, Sasaki S, Shirasu M. 1993. Milky spots as the implantation site for malignant cells in peritoneal dissemination in mice. *Cancer Res.* 53: 687-692.
13. Hogquist KA, Jameson SC, Heath WR, Howard JL, Bevan MJ, Carbone FR. 1994. T cell receptor antagonist peptides induce positive selection. *Cell* 76: 17-27.
14. Clarke SR, Barnden M, Kurts C, Carbone FR, Miller JF, Heath WR. 2000. Characterization of the ovalbumin-specific TCR transgenic line OT-I: MHC elements for positive and negative selection. *Immunol. Cell Biol.* 78: 110-117.
15. Barnden MJ, Allison J, Heath WR, Carbone FR. 1998. Defective TCR expression in transgenic mice constructed using cDNA-based α- and β-chain genes under the control of heterologous regulatory elements. *Immunol. Cell Biol.* 76: 34-40.
16. Gorer PA. 1950. Studies in antibody response of mice to tumour inoculation. *Br. J. Cancer* 4: 372-379.
17. Moore MW, Carbone FR, Bevan MJ. 1998. Introduction of soluble protein into the class I pathway of antigen processing and presentation. *Cell* 54: 777-785.
18. Mizuochi T, Loveless RW, Lawson AM, Chai W, Lachmann PJ, Childs RA, Thiel S, Feizi T. 1989. A library of oligosaccharide probes (neoglycolipids) from N-glycosylated proteins reveals that conglutinin binds to certain complex-type as well as high mannose-type oligosaccharide chains. *J. Biol. Chem.* 264: 13834-13839.
19. Shimizu Y, Takagi H, Nakayama T, Yamakami K, Tadakuma T, Yokoyama N, Kojima N. 2007. Intraperitoneal immunization with oligomannose-coated liposome-entrapped soluble leishmanial antigen induces antigen-specific T-helper type 1 immune response in BALB/c mice through uptake by peritoneal macrophages. *Parasite Immunol.* 29: 229-239.
20. Takagi H, Furuya N, Kojima N. 2007. Preferential production of IL-12 by peritoneal macrophages activated by liposomes prepared from neoglycolipids containing oligomannose residues. *Cytokine* 40: 241-250.

21. Kato C, Kajiwara T, Numazaki M, Takagi H, Kojima N. 2008. Oligomannose-coated liposomes activate ERK via Src kinases and PI3K/Akt in J774A.1 cells. *Biochem. Biophys. Res. Commun.* 372: 898-901.
22. Abe Y, Kuroda Y, Kuboki N, Matsushita M, Yokoyama N, Kojima N. 2008. Contribution of complement component C3 and complement receptor type 3 to carbohydrate-dependent uptake of oligomannose-coated liposomes by peritoneal macrophages. *J. Biochem.* 144: 563-570.
23. Takagi H, Numazaki M, Kajiwara T, Abe Y, Ishii M, Kato C, Kojima N. 2009. Cooperation of specific ICAM-3 grabbing nonintegrin-related 1 (SIGNR1) and complement receptor type 3 (CR3) in the uptake of oligomannose-coated liposomes by macrophages. *Glycobiology* 19: 258-266.
24. Armstrong DK, Bundy B, Wenzel L, Huang HQ, Baergen R, Lele S, Copeland LJ Walker JL, Burger RA, Gynecologic Oncology Group. 2006. Intraperitoneal cisplatin and paclitaxel in ovarian cancer. *N. Engl. J. Med.* 354: 34-43.
25. Kojima N, Biao L, Nakayama T, Ishii M, Ikehara Y, Tsujimura K. 2008. Oligomannose-coated liposomes as a therapeutic antigen-delivery and an adjuvant vehicle for induction of in vivo tumor immunity. *J. Control. Release* 129: 26-32.

The cellular niche of *Listeria monocytogenes* infection changes rapidly in the spleen

Taiki Aoshi[1], *Javier A. Carrero*[1], *Vjollca Konjufca*[1], *Yukio Koide*[2], *Emil R. Unanue*[1] *and Mark J. Miller*[1]

[1] Department of Pathology and Immunology, Washington University School of Medicine, St. Louis, MO, USA
[2] Department of Infectious Diseases, Hamamatsu University School of Medicine, Hamamatsu, Shizuoka, Japan

The spleen is an important organ for the host response to systemic bacterial infections. Many cell types and cell surface receptors have been shown to play role in the capture and control of bacteria, yet these are often studied individually and a coherent picture has yet to emerge of how various phagocytes collaborate to control bacterial infection. We analyzed the cellular distribution of *Listeria monocytogenes* (LM) *in situ* during the early phase of infection. Using an immunohistochemistry approach, five distinct phagocyte populations contained LM after i.v. challenge and accounted for roughly all bacterial signal in tissue sections. Our analysis showed that LM was initially captured by a wide range of phagocytes in the marginal zone, where the growth of LM appeared to be controlled. The cellular distribution of LM within phagocyte populations changed rapidly during the first few hours, decreasing in marginal zone macrophages and transiently increasing in CD11c$^+$ DC. After 4–6 h LM was transported to the periarteriolar lymphoid sheath where the infective foci developed and LM grew exponentially.

Key words: Bacterial infection · DC · *Listeria monocytogenes* · Macrophages · Spleen

Supporting Information available online

Introduction

The spleen is an important site for host responses to bacterial infection [1, 2]. Within the spleen, bacteria may encounter various tissue resident phagocytes including macrophages, DC, and neutrophils [3, 4]. Marginal zone macrophages (MZM) are positioned along the outer layer of the marginal sinus where they have direct access to bacteria entering the spleen from the circulation. These macrophages express MARCO (macrophage receptor with collagenous structure), a type-1 scavenger receptor, related to the SR-A family of receptors [5], which recognizes bacterial cell-wall-associated polyanions [6]. MZM also express the C-type lectin, SIGN-R1. SIGN-R1 binds dextran [7] and facilitates the capture of polysaccharide antigens on bacteria such as *Streptococcus pneumoniae* [8]. A separate class of MZM, the metallophilic MZM (MMM), localize between the inner marginal sinus and the B-cell follicle [9]. These cells recognize sialic acid and LPS from *Neiseria meningitidis* [10] through Siglec-1 (sialic-acid-binding-Ig-like-lectin 1) [11, 12]. MMM have also been shown to produce interferon during Herpes simplex virus infection [13], but their role in bacterial infection is unclear, although it was reported that they produce CCL2 [14].

Neutrophils play a crucial role in controlling bacterial infection [15–19]. They are present in the marginal zone (MZ) and

Correspondence: Dr. Mark J. Miller
e-mail: miller@pathology.wustl.edu

red pulp (RP) of the spleen and therefore have access to circulating bacteria and bacteria released from infected splenocytes. Also within the MZ of the spleen resides a population of DC recognized with the antibody 33D1 [20], which have been shown to efficiently present antigens to $CD4^+$ T cells [21]. The location of these cells in the MZ suggests that they may participate in the capture of bacteria in the circulation. Macrophages are also present in the RP [22]. These macrophages are $F4/80^+$ and primarily serve to remove dying red blood cells and other debris from the circulation [23].

We used intravenous LM infection [24] and a semi-quantitative immunofluorescence approach to investigate the capture and clearance of bacteria in the spleen. Previous histological studies showed that LM was trapped in the MZ of the spleen [25–27]. Clodronate-liposome depletion of MZ macrophages *in vivo* indicated that they were required for initial LM capture and control, but were dispensable for specific T-cell-mediated immunity [25]. At 24 h following infection, LM was found primarily within $CD11b^+$ and, to a less extent, $CD11c^+$ cells [27]. More recently, $CD8\alpha^+$ DC were found to be the primary cell type containing viable bacteria early after infection (1–3 h) [28]. Other studies have detected LM exclusively in SIGN-$R1^+$ MZM and not $CD11c^+$ DC very early after infection [14]. Here, we identified five phagocyte populations that contained the bulk of LM after i.v. challenge. During the time when LM was in the MZ, its colocalization with MZM decreased dramatically. This shift in the cellular niche of LM *in vivo* has important implications for bacterial pathogenesis and protective host responses in the spleen.

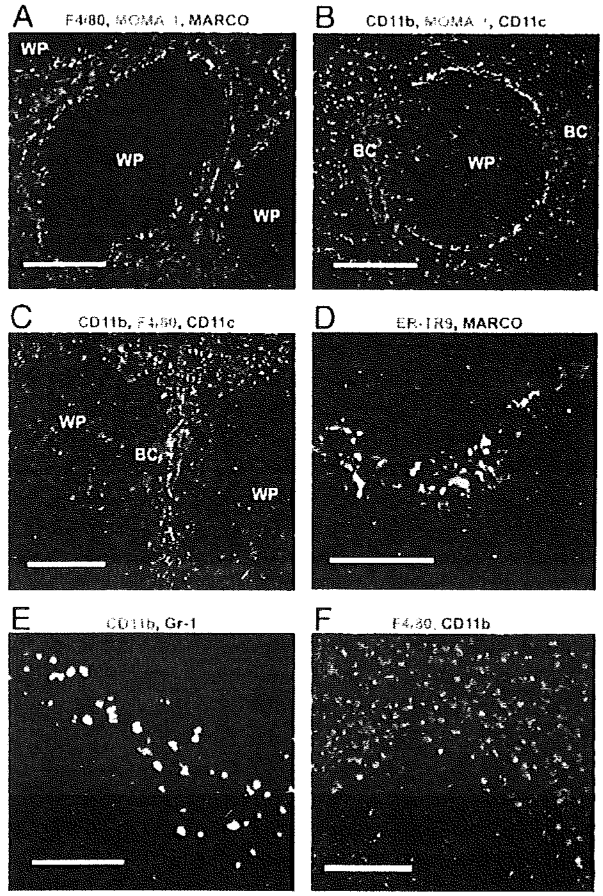

Figure 1. Histological characterization of resident phagocytes in the spleen. Cryosections from normal BALB/c mice were stained with different combinations of host cell markers to demonstrate staining specificity. (A) Anti-F4/80 (blue), anti-MOMA-1 (green), and anti-MARCO (red). (B) Anti-CD11b (blue), MOMA-1 (green), and CD11c (red). (C) Anti-CD11b (blue), anti-F4/80 (green), and anti-CD11c (red). (D) Anti-ER-TR9 (green) and anti-MARCO (red). Nearly all ER-$TR9^+$ cells also express MARCO (yellow), suggesting that they are a subset of the $MARCO^+$ MZM. (E) Anti-Gr-1 (green) and anti-CD11b (red). Approximately, 95% of $CD11b^+$ cells are small, round and co-stained with Gr-1. (F) $CD11b^+$ cells do not stain with F4/80, anti-F4/80 (green) and anti-CD11b (red). Scale bar = 200 μm in (A–C) and 100 μm in (D–F). Images are representative of three independent experiments. WP: white pulp. BC: bridging channel.

Results

LM enters a wide variety of phagocytes immediately after challenge

We found that the recovery of LM (EGD)-infected host cells from spleen was unreliable; ~90% of LM CFU were lost in the process of isolating phagocytes and making single cell suspensions (Supporting Information Fig. 1). As an alternative, we developed an antibody staining approach, by which we identified five distinct phagocyte populations in spleen cryosections (Fig. 1 and Supporting Information Fig. 2). We observed three distinct macrophage subsets in their expected locations: $F4/80^+$ in the RP, $MARCO^+$ MZM in the outer MZ, and MOMA-1^+ MMM in the inner MZ (Fig. 1A–C) [5, 9, 22, 29]. Nearly all ER-$TR9^+$ MZM co-stained with antibodies to MARCO, suggesting that SIGN-$R1^+$ cells are actually a subset of $MARCO^+$ MZM (Fig. 1D). The $CD11b^{hi}$ cells in our images appeared to be neutrophils, since they were smaller and rounder than macrophages and localized outside the white pulp (Fig. 1B, C, and F). Moreover, >95% of $CD11b^+$ cells were Gr-1^+ (Ly6G) and $F4/80^-$ in co-stained sections (Fig. 1E and F). However, Gr-1 also reacts with the epitope Ly6C expressed on a number of other cell types, including inflammatory macrophages, making it difficult to define the $CD11b^+$ population unambiguously. We found $CD11c^+$ cells localized to the periarteriolar lymphoid sheath (PALS), the bridging channel and distributed sparsely in the RP and the MZ (Fig. 1B and C), also consistent with previous reports [30–32].

To reveal the host cells that interacted with LM immediately after infection, mice were injected with LM and sacrificed from minutes to hours later. Cryosections were prepared, stained with antibodies to LM and various host cell markers and the percentage of LM fluorescence signal overlap with each phagocyte surface marker (*i.e.* colocalization coefficient) was determined as described previously [33] (Fig. 2).

In contrast to previous reports [14, 28], LM entered a wide range of host phagocytes in the spleen (Fig. 2A). The percentage of LM signal colocalized with each host cell type was as follows: F4/80$^+$ macrophages (26%), MARCO$^+$ macrophages (30%), MOMA-1$^+$ macrophages (19%), CD11b$^+$ cells (18%), and CD11c$^+$ DC (18%) and B220$^+$ cells (10%) (Fig. 2B). We included B220 staining as an internal negative control, because lymphocytes including B cells are not directly infected by LM. LM colocalization with B220 ranged from 5 to 10% in individual experiments. However, the covariance of LM and B220 signal was consistently negative (Pearson's correlation coefficient = −0.25), indicating that colocalization was less than that expected by chance alone, thus making B220 a suitable negative control. (The B220 stain may include plasmacytoid DC (pDC), but their contribution should be negligible since they represent less than 1% of spleen cells while B cells represent close to 50%.)

Histological analyses were performed at different concentrations of LM including those over the LD_{50} dose (Fig. 2C). At the 10^6 dose, most phagocytes contained a single bacterium (Fig. 2A). At a higher dose (10^8), increased variation was observed with many cells containing one LM and others containing small clusters of LM (Fig. 2C). Despite a 100-fold increase in dose (from 10^6 to 10^8), the cellular distribution of LM remained remarkably similar at 30 min after injection (compare panel 2D with 2B in Fig. 2), with the exception that more LM was found in CD11b$^+$ cells with the larger inocula (38% up from 18%). We also gave mice a 20-fold lower dose of LM (5×10^4) and examined its distribution. Although the number of bacteria in each section was small and highly variable, we found numerous examples of LM colocalized to each of the five phagocyte populations (Supporting Information Fig. 3A and B), similar to experiments using 10^6 LM.

We also examined the colocalization of bacteria in a sublethal infection using attenuated LM strain MORO-2 ($LD_{50} \sim 3 \times 10^6$) [34], which behaves normally during the first few hours of infection, but can replicate only approximately three times in the host cytosoplasm due to a deficiency in lipoic acid utilization. The cellular distribution of 10^6 MORO-2 was indistinguishable from experiments using 10^6 EGD (Supporting Information Fig. 3C and D).

Next, we compared LM uptake with other known substrates of phagocytosis: fluorescent polystyrene beads and FITC-conjugated dextrans. At 30 min after injection, fluorescent beads were taken up by MZM and, to a much lesser extent, by CD11c$^+$ DC (Fig. 2E). The majority of beads (~76%) were associated with MARCO$^+$ cells, ~40% with MOMA-1$^+$ MMM, and < 20% with CD11c$^+$ DC. Few, if any, beads were associated with CD11b$^+$ and F4/80$^+$ cells. FITC-conjugated dextran, which has been shown to be taken up specifically by MZM (MARCO$^+$ ER-TR9$^+$) *via* SIGN-R1 [7], was captured efficiently by MARCO$^+$ cells and accumulated to high levels by 30 min (Fig. 2F). The other phagocyte populations examined showed only background levels of colocalization with dextran (Fig. 2F), validating our analysis. Thus, the trapping of LM was unexpectedly promiscuous compared with the uptake of fluorescent beads and dextran.

It is important to note that the initial trapping compartment of LM was capable of controlling infection. We have infected wild-type 129/SvEv, as well as type I and type II interferon-deficient mice (IFNAR and IFNGR) and found limited to no growth of bacteria between 30 min and 4 h post-infection in the spleen (Fig. 2G). This would suggest that the net ability of the MZ cells is to control LM independent of tonic interferon signaling.

The cellular niche of LM changes rapidly

The fate of LM in phagocytes was examined during the first hours of infection. From 30 min to 6 h, the amount of LM *per* cell in F4/80$^+$ and CD11c$^+$ cells held steady without an appreciable increase (Fig. 3A). For MOMA-1$^+$ cells, a slight increase at 2 h was observed; however, there was no significant difference between 30 min and 6 h. In contrast, LM signal in MARCO$^+$ and CD11b$^+$ cells decreased significantly (Fig. 3A). To determine whether this result also held true for ER-TR9$^+$ MZM, we examined LM colocalization with ER-TR9 (bright yellow spots in Fig. 3B) and found it decreased significantly at 2 and 6 h (Fig. 3B and C). In addition, we observed a marked decrease in covariance between LM and ER-TR9 signals over the first 6 h after infection (Fig. 3D). The total LM pixel *per* image remained relatively stable over this time (Fig. 3E) and was well correlated to the actual CFU counts *per* spleen (Fig. 3F). Moreover, host cell signal remained constant, with the exception of CD11b, which increased roughly 50% between 30 min and 6 h (Fig. 3G). We believe that the increased in CD11b$^+$ signal most likely represents the infiltration of cells because the signal increases rapidly and we did not detect a gradual rise in signal intensity on a *per* cell basis between 0.5 and 6 h (data not shown). After 6 h, LM is also detected in the PALS, the site of rapid exponential growth of LM in the spleen [27, 35].

At 12 h, approximately 40% of the LM signal in the MZ was found in CD11c$^+$ cells (Fig. 4A), while about 20% was found in each of the F4/80$^+$, MOMA-1$^+$, and CD11b$^+$ populations, similar to the 30 min time point. In contrast, only 5% of the LM signal was found in MARCO$^+$ MZM (compared with 30% at 30 min). By 24 h, when LM infection was confined primarily to the PALS, the cellular distribution of LM changed further (Fig. 4B). The majority of infected cells at 24 h were CD11b$^+$ cells (54%) and LM was barely detectable in MARCO$^+$ MZM (~2% colocalization). The percentage of colocalization with CD11c$^+$ cells also fell sharply to 22%. Both, F4/80$^+$ macrophages and MOMA-1$^+$ cells continued to show evidence of LM infection with colocalization coefficients of 17 and 18%, respectively.

Discussion

Defining the cellular niche occupied by bacteria in the spleen is fundamental for understanding how bacterial pathogenesis proceeds *in vivo* and how the host mounts a protective immune response. Our analysis showed that LM was taken up initially by a broad range of phagocytic cells, including macrophages (MARCO$^+$, ERT-R9$^+$, and F4/80), granulocytes (CD11b$^+$, Gr-1$^+$ cells) and DC (CD11c$^+$), in general agreement with a previous histological study [26]. These results contrast sharply with the conclusions of others that LM was captured exclusively by CD8a$^+$ DC [28] or

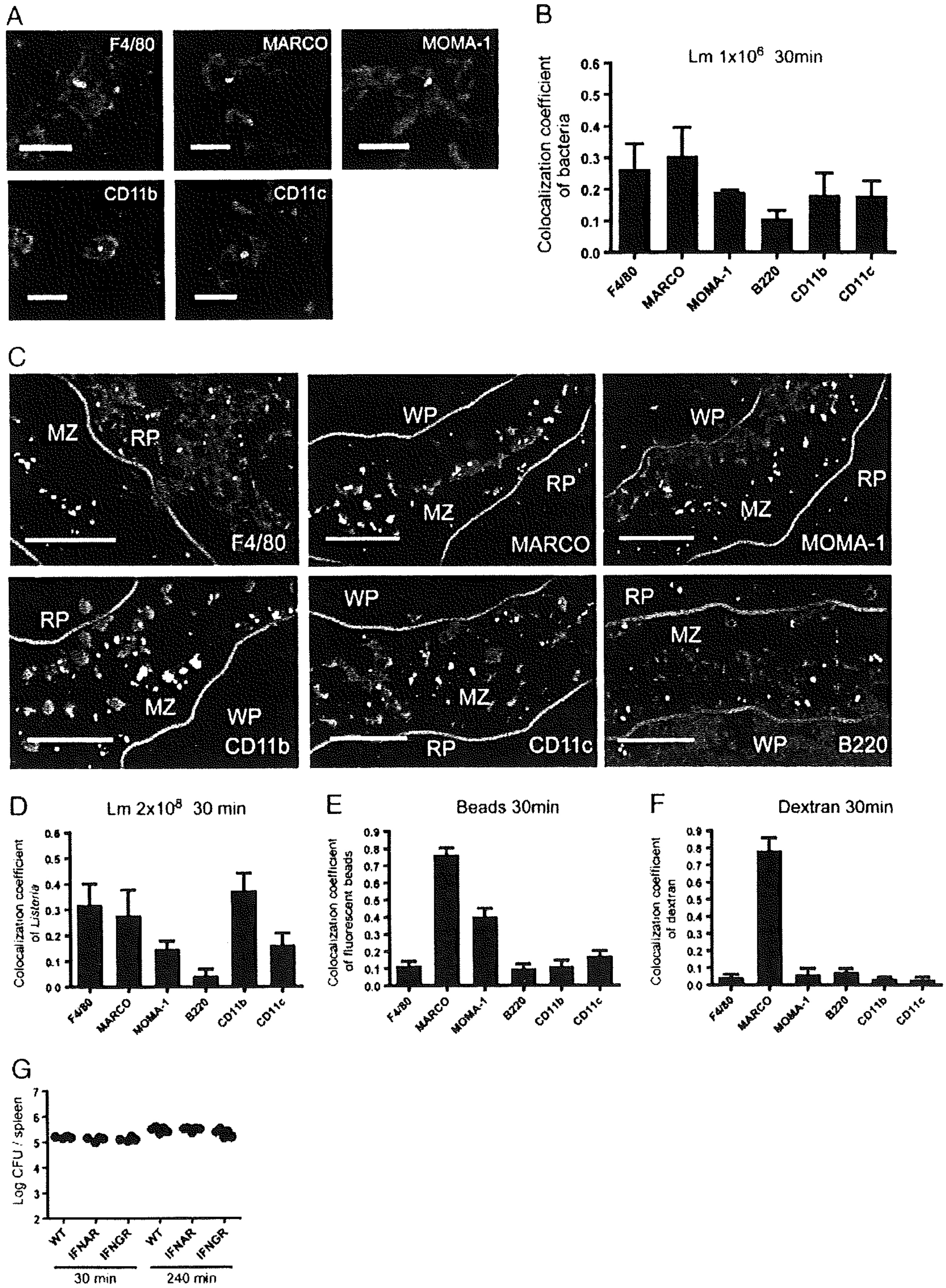

Figure 2. LM is broadly distributed in splenocytes immediately after i.v. infection. (A) Infected host cells in stained cryosections 30 min following infection with 10^6 EGD strain of LM. LM (green) and host cell markers (red). Scale bar = 10 μm. Images are representative of three independent experiments. (B) LM colocalization with host cell types. Bars represent mean+SD of at least 30 images *per* each cell type. (C) Spleens at 30 min post infection with 2×10^8 LM. Cryosections were stained with phalloidin-Alexa Fluor 350, anti-LM (green) and indicated host cell markers (red). Yellow represents colocalization between LM and stained host-cells. Blue lines represent the edge of the MZ determined by phalloidin staining. Scale bar = 50 μm. (D) Colocalization analysis of (D) 2×10^8 LM, (E) 7.2×10^8 fluorescent 1.0 μm beads, and (F) 200 μg of 70 kDa FITC-conjugated dextran with splenic phagocytes 30 min after i.v. injection. Bars represent mean+SD of ten images *per* cell type. (G) 129/SvEv, IFNAR, and IFNGR mice were infected intravenously with 10^7 CFU of LM EGD strain and spleen colony counts were determined at 30 and 240 min post infection. MZ: marginal zone; RP: red pulp; WP: white pulp.

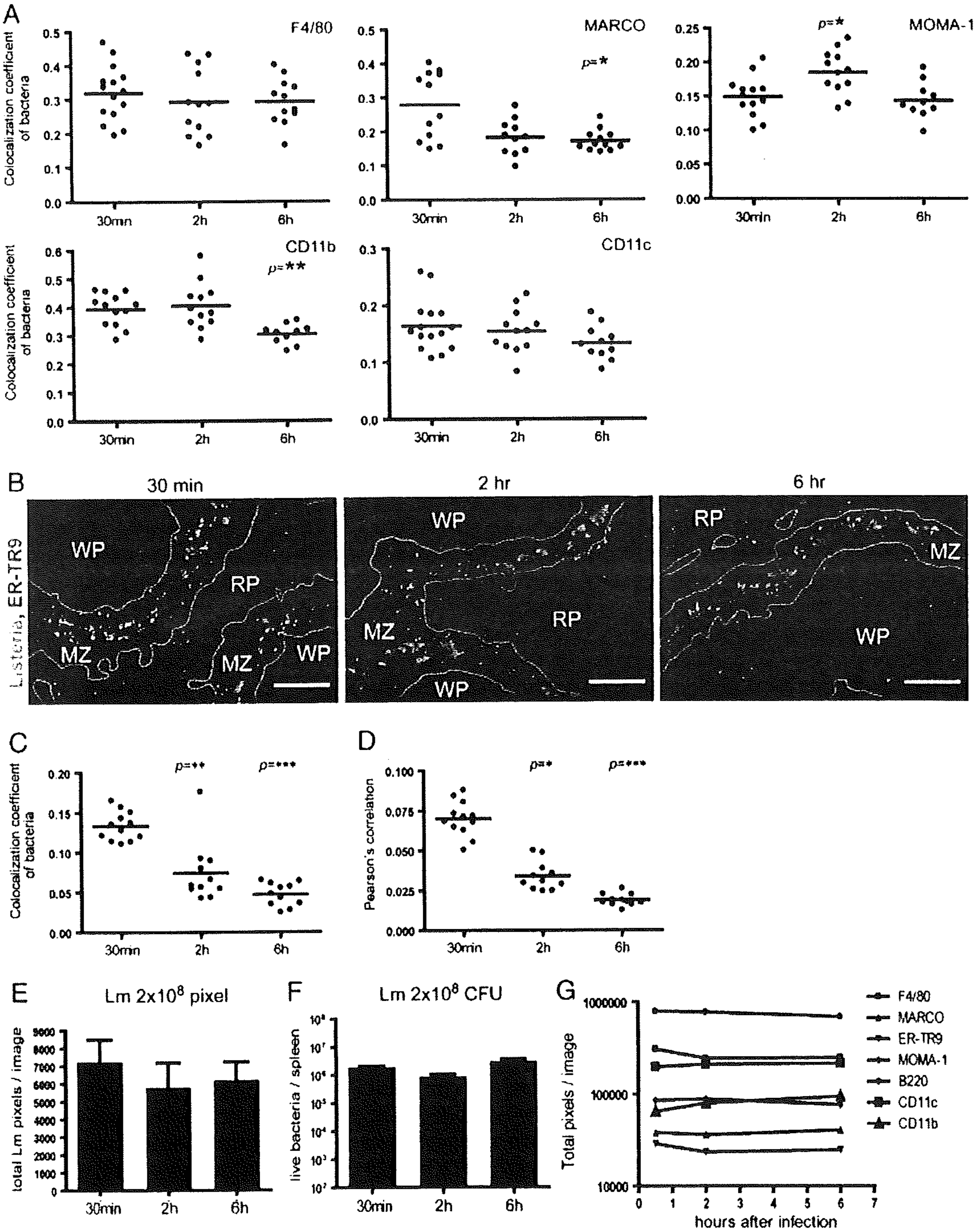

Figure 3. LM signal decreases in MZM 0.5–6 h post-infection. (A) The colocalization coefficients of LM and host cell markers over time. Scatter plots show mean values for individual images and pooled means. (B) Spleen sections from mice infected with 2×10^8 LM at 30 min, 2 h, and 6 h. Cryosections were stained with phallodin-Alexa Fluor 350, anti-LM (green) and anti-SIGNR1 (red). Colocalization between LM and host-cells appears yellow in the image. Blue lines highlight the MZ edge drawn based on phalloidin staining. Scale bar = 100 µm. Images are representative of ten images *per* time point. (C) Colocalization of LM in ER-TR9$^+$ cells and (D) covariance of LM and ER-TR9 signal (Pearson's correlation), at increasing times after infection. Each dot is the mean value of a single image and pooled means are shown. (E) LM signal in pixels *per* image at 30 min, 2 h, and 6 h post infection (2×10^8 LM). Bars show mean+SD of 50 images *per* time point. (F) CFU *per* spleen 30 min, 2 h, and 6 h post infection (2×10^8 LM). Bars show mean+SD, five mice *per* group. (G) Host cell signal expressed in pixels *per* image at increasing times after infection. Graph shows mean of 12 images *per* group. All data are representative of three independent experiments with similar results. MZ: marginal zone; RP: red pulp; WP: white pulp.

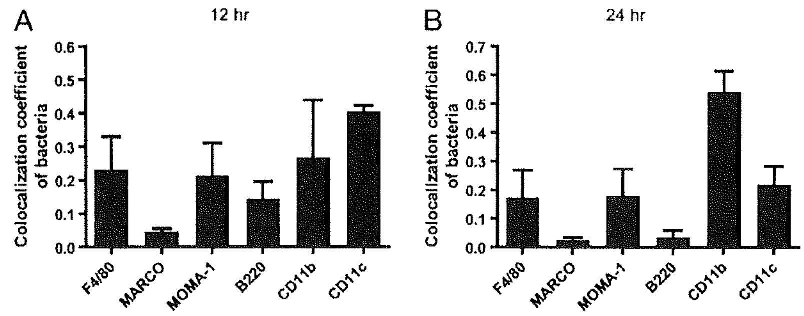

Figure 4. Host cell distribution of LM 12 and 24 h post infection. LM colocalization with splenic phagocytes 12 h (A) and 24 h (B) after infection. Bars represent mean+SD of ten images *per* cell type. Bar graphs are representative of three independent experiments. LM disappears rapidly from MARCO$^+$ MZM, but increases transiently in CD11c$^+$ cells.

ER-TR9$^+$ macrophages [14]. Histological studies from independent groups concur that LM associates with resident macrophages in the MZ for several hours after infection, although the characterization of macrophages differed depending on the markers used to detect them [14, 25–27]. Neuenhahn *et al.* [28] detected only viable LM present in splenocytes isolated by cell sorting, but because MZM are difficult to recover from spleen tissue, these cells could be easily missed during data analysis.

We used a panel of five different antibodies to provide a comprehensive histological view of early LM infection in the spleen. The criteria for including antibodies in our analysis were (i) staining must be highly reproducible and the results entirely consistent with classical histological studies with regard to the morphology and anatomical location of splenic DC, MZM, metallophilic macrophages, granulocytes, and lymphocytes [4, 9, 31, 32, 36, 37], (ii) antibodies must stain distinct splenocyte populations with minimal overlap (verified by co-staining), and (iii) the percent colocalization with LM and each host cell marker must be reproducible and the colocalized LM signal must add up to ~100% of the total LM signal in our sections (*i.e.* to ensure that no major splenocyte populations are missed). Our analysis focused on the early stages of LM infection but it will be important to examine other splenocyte populations such as inflammatory monocytes, pDC, and tumor necrosis factor alpha and inducible nitric oxide synthase producing DC (Tip DC) [38, 39] at later times.

In addition, we assessed the robustness of our colocalization analysis with several control experiments. We found dextran colocalized strongly with MZM (MARCO$^+$), but not other phagocytes, consistent with the fact that MZM express the dextran receptor SIGN-R1 [5]. Fluorescent beads were taken up by MARCO$^+$ and MOMA-1$^+$ macrophages, to a much lesser extent by CD11c$^+$ cells and were undetectable in CD11b$^+$ cells. The initial cellular niche of LM was strikingly promiscuous and our data suggest that LM might enter host cells *via* multiple receptors and phagocytic pathways.

During the first 4–6 h, when bacteria are located primarily in the MZ, LM growth appeared to be controlled. It was not only until LM was transported to the PALS that the exponential phase of LM growth took place. During this period the host cell distribution changed: the number of LM in MARCO$^+$ (and ER-TR9$^+$) macrophages decreased during the first few hours of infection, while it persisted in other cell types, such as CD11c$^+$ DC and MOMA-1$^+$ MMM. Whether the apparent control reflects a cytocidal activity of the MZM or is a reflection of cellular dynamics and turnover is not clear at this time. However, the capture of LM by MZM is undoubtedly important since clodronate-liposome depletion of these phagocytes augmented infection. Experiments are in progress to elucidate the mechanisms of LM control in the MZ, but our initial studies (Fig. 2G) indicate that this control is independent of either interferon-gamma or type-1 interferons. To note is that MARCO- and SIGN-R1-deficient mice were highly susceptible to pneumococcal infection [8, 40]. It will be interesting to compare and contrast LM infection with other bacteria such as *Staphylococcus* and *Salmonella* to determine whether the MZ control extends across bacterial species and possibly to viruses, as seen in LCMV infection [41, 42]. It is noteworthy that although RP macrophages do not appear to be listericidal, they apparently fail to support the proliferation of LM, since we did not detect an increase in the amount of LM in the F4/80$^+$ cells during the timeframe of our experiments.

In contrast to the MZ stage of infection, LM signal increased explosively in the PALS from 12-24 h. The preferential replication of LM in the PALS might reflect decreased bactericidal capacity or alternatively PALS resident cells, such as DC, might be more permissive for LM proliferation. In fact, we observed a significant increase of LM in DC over the first 12 h of infection. Moreover the heightened and very extensive lymphocyte apoptosis in PALS has been shown to be in great part responsible for such strong expansion of LM [43].

Materials and methods

Mice

BALB/cJ mice were obtained from the Jackson Laboratory (Bar Harbor, ME) and were maintained and bred under specific pathogen free conditions in the Washington University mouse facility, in accordance with the guidelines of the Washington

University Committee for the Humane Care of Laboratory Animals and with National Institutes of Health guidelines on laboratory animal welfare.

Bacteria and fluorescent reagents

LM strain EGD was stored as frozen glycerol stocks ($\sim 1 \times 10^9$/mL) at −80°C. LM numbers in the spleen were estimated by determining CFU from tissue homogenates using standard procedures. For early time point experiments (30 min–6 h), bacteria were cultured in BHI medium and harvested during log phase growth for inoculation. LM concentrations in liquid cultures were estimated by optical density measurements using standard growth curves. For 12 and 24 time points, frozen stocks were thawed and diluted appropriately prior to i.v. injection. Our frozen stocks contained negligible dead bacteria (96.88% viability, $p = 0.48$) compared with starting cultures for up to 5 months. FluoSpheres carboxylate-modified microspheres (yellow green, 1.0 μm) and Fluorescein-conjugated dextran (lysine-fixable, 70 kDa) were purchased from Invitrogen (Carlsbad, CA).

Histology

Spleens were harvested, embedded in OCT compound and 5 μm cryosections were prepared. Sections were fixed with 4% paraformaldehyde in PBS (pH 7.2) at 4°C for 5 min and blocked with StartingBlock Blocking Buffer (Thermo Fisher Scientific, Rockford, IL) for 10 min, then sequentially incubated with purified and/or biotin-conjugated primary antibodies and fluorescent-dye-conjugated secondary antibodies and/or fluorescent-dye-conjugated streptavidin. Antibodies and reagents used for staining were as follows: phalloidin-Alexa Fluor 350 (Invitrogen), rat anti-mouse F4/80 (biotin conjugated, BM8; eBioscience, San Diego, CA),

Rat anti-mouse/human CD45R/B220 (PE or Alexa Fluor 647 conjugated, RA3-6B2; eBioscience, or BD Biosciences, San Jose, CA), rat anti-mouse MARCO (PE-conjugated, ED31; Serotec, Oxford, UK), rat anti-mouse SIGN-R1 (biotin-conjugated, ER-TR9; BMA Biomedicals, Augst, Switzerland).

Rat anti-mouse siglec-1 (biotin or FITC-conjugated, MOMA-1; BMA Biomedicals or Serotec), hamster anti-mouse CD11c (biotin or PE-conjugated, HL3 or N418; BD Biosciences or eBioscience), rat anti-mouse CD11b (biotin, Alexa Fluor 647 or PE-conjugated, M1/70; BD Biosciences or eBioscience), rabbit anti-LM polyserum serotypes 1 and 4 (BD Diagnostic Systems, Sparks, MD), goat anti-rabbit IgG (FITC-conjugated; Sigma, St. Louis, MO), streptavidin (Alexa Fluor 555 or Alexa Fluor 647-conjugated; Invitrogen), rat anti-mouse Ly-6G(Gr-1) (PE-conjugated, RB6-8C5; eBioscience).

Immunofluorescence microscopy

Four-color fluorescence microscopy of cryosections was performed using an Olympus BX51 equipped with 100 W mercury lamp (Olympus America, Center Valley, PA) and a SPOT RT charge-coupled device camera (Diagnostic Instruments, Sterling Heights, MI). Monochrome images (1200 pi × 1600 pi = 885 × 1180 μm in 10× objectives; 440 × 586 μm in 20× objectives, 12-bit ;depth) were acquired with filter sets optimized for DAPI, FITC, tetramethyl rhodamine isothiocyanate (TRITC), and cyanine dye 5 (Cy5, 670 nm emission), respectively (Chroma, Rockingham, VT). Exposure times of 1–2 s were used and a linear contrast stretch was applied to the images to normalize brightness. Monochrome images were pseudo-colored and merged into 24 bit RGB images with SPOT RT camera software and exported into Adobe Photoshop for subsequent color balancing and image segmentation. Colocalization coefficients and Pearson's correlation coefficients [33] were generated from pooled fluorescent images with Volocity software (version 3.7; Improvision, Waltham, MA). Color-balanced images were transferred to Volocity and RGB channels were split. Thresholds were set for each channel using automatic thresholding and were confirmed by eye; in cases where automatic thresholding failed, thresholds were re-adjusted manually comparable to other images. All data from three time points (30 min, 2 h, and 6 h) were first tested with One-way ANOVA (Kruskal–Wallis test, nonparametric). If the overall p-value was < 0.05, 30 min *versus* 2 h, and 30 min *versus* 6 h were secondarily tested with the Dunns test. *$p<0.05$, **$p<0.01$, ***$p<0.001$.

Acknowledgements: The authors thank Xin Zhang for the breeding and care of the mice used in this study and Bernd H. Zinselmeyer and Jennifer N. Lynch for helpful comments on the paper. The authors also thank Mary O'Riordan for providing the MORO-2 LM strain. This work was supported in part by a grant from the National Institutes of Health (AI062832, ERU).

Conflict of interest: The authors declare no financial or commercial conflict of interest.

References

1 **Junt, T., Scandella, E. and Ludewig, B.**, Form follows function: lymphoid tissue microarchitecture in antimicrobial immune defence. *Nat. Rev. Immunol.* 2008. 8: 764–775.

2 **Khanna, K. M. and Lefrançois, L.**, Geography and plumbing control the T cell response to infection. *Immunol. Cell Biol.* 2008. 86: 416–422.

3 **Kraal, G.**, Cells in the marginal zone of the spleen. *Int. Rev. Cytol.* 1992. 132: 31–74.

4 **Mebius, R. E. and Kraal, G.**, Structure and function of the spleen. *Nat. Rev. Immunol.* 2005. 5: 606–616.

5 **Elomaa, O., Kangas, M., Sahlberg, C., Tuukkanen, J., Sormunen, R., Liakka, A., Thesleff, I. et al.**, Cloning of a novel bacteria-binding receptor structurally related to scavenger receptors and expressed in a subset of macrophages. *Cell* 1995. 80: 603–609.

6 Sankala, M., Brannstrom, A., Schulthess, T., Bergmann, U., Morgunova, E., Engel, J., Tryggvason, K. and Pikkarainen, T., Characterization of recombinant soluble macrophage scavenger receptor MARCO. *J. Biol. Chem.* 2002. **277**: 33378–33385.

7 Kang, Y. S., Yamazaki, S., Iyoda, T., Pack, M., Bruening, S.A., Kim, J. Y., Takahara, K. *et al.*, SIGN-R1, a novel C-type lectin expressed by marginal zone macrophages in spleen, mediates uptake of the polysaccharide dextran. *Int. Immunol.* 2003. **15**: 177–186.

8 Lanoue, A., Clatworthy, M. R., Smith, P., Green, S., Townsend, M. J., Jolin, H. E., Smith, K. G. *et al.*, SIGN-R1 contributes to protection against lethal pneumococcal infection in mice. *J. Exp. Med.* 2004. **200**: 1383–1393.

9 Kraal, G. and Janse, M., Marginal metallophilic cells of the mouse spleen identified by a monoclonal antibody. *Immunology* 1986. **58**: 665–669.

10 Jones, C., Virji, M. and Crocker, P. R., Recognition of sialylated meningococcal lipopolysaccharide by siglecs expressed on myeloid cells leads to enhanced bacterial uptake. *Mol. Microbiol.* 2003. **49**: 1213–1225.

11 Oetke, C., Kraal, G. and Crocker, P. R., The antigen recognized by MOMA-I is sialoadhesin. *Immunol. Lett.* 2006. **106**: 96–98.

12 Crocker, P. R., Kelm, S., Dubois, C., Martin, B., McWilliam, A. S., Shotton, D. M., Paulson, J. C. and Gordon, S., Purification and properties of sialoadhesin, a sialic acid-binding receptor of murine tissue macrophages. *EMBO J.* 1991. **10**: 1661–1669.

13 Eloranta, M. L. and Alm, G. V., Splenic marginal metallophilic macrophages and marginal zone macrophages are the major interferon-alpha/beta producers in mice upon intravenous challenge with herpes simplex virus. *Scand. J. Immunol.* 1999. **49**: 391–394.

14 Jablonska, J., Dittmar, K. E., Kleinke, T., Buer, J. and Weiss, S., Essential role of CCL2 in clustering of splenic ERTR-9+macrophages during infection of BALB/c mice by *Listeria monocytogenes*. *Infect. Immun.* 2007. **75**: 462–470.

15 Nathan, C., Neutrophils and immunity: challenges and opportunities. *Nat. Rev. Immunol.* 2006. **6**: 173–182.

16 Conlan, J. W. and North, R. J., Neutrophils are essential for early anti-Listeria defense in the liver, but not in the spleen or peritoneal cavity, as revealed by a granulocyte-depleting monoclonal antibody. *J. Exp. Med.* 1994. **179**: 259–268.

17 Czuprynski, C. J., Brown, J. F., Maroushek, N., Wagner, R. D. and Steinberg, H., Administration of anti-granulocyte mAb RB6-8C5 impairs the resistance of mice to *Listeria monocytogenes* infection. *J. Immunol.* 1994. **152**: 1836–1846.

18 Rogers, H. W. and Unanue, E. R., Neutrophils are involved in acute, nonspecific resistance to *Listeria monocytogenes* in mice. *Infect. Immun.* 1993. **61**: 5090–5096.

19 Unanue, E. R., Inter-relationship among macrophages, natural killer cells and neutrophils in early stages of Listeria resistance. *Curr. Opin. Immunol.* 1997. **9**: 35–43.

20 Witmer, M. D. and Steinman, R. M., The anatomy of peripheral lymphoid organs with emphasis on accessory cells: light-microscopic immunocytochemical studies of mouse spleen, lymph node, and Peyer's patch. *Am. J. Anat.* 1984. **170**: 465–481.

21 Dudziak, D., Kamphorst, A. O., Heidkamp, G. F., Buchholz, V. R., Trumpfheller, C., Yamazaki, S., Cheong, C. *et al.*, Differential antigen processing by dendritic cell subsets *in vivo*. *Science* 2007. **315**: 107–111.

22 Austyn, J. M. and Gordon, S., F4/80, a monoclonal antibody directed specifically against the mouse macrophage. *Eur. J. Immunol.* 1981. **11**: 805–815.

23 Oldenborg, P. A., Zheleznyak, A., Fang, Y. F., Lagenaur, C. F., Gresham, H. D. and Lindberg, F. P., Role of CD47 as a marker of self on red blood cells. *Science* 2000. **288**: 2051–2054.

24 Pamer, E. G., Immune responses to *Listeria monocytogenes*. *Nat. Rev. Immunol.* 2004. **4**: 812–823.

25 Aichele, P., Zinke, J., Grode, L., Schwendener, R. A., Kaufmann, S. H. and Seiler, P., Macrophages of the splenic marginal zone are essential for trapping of blood-borne particulate antigen but dispensable for induction of specific T cell responses. *J. Immunol.* 2003. **171**: 1148–1155.

26 Conlan, J. W., Early pathogenesis of *Listeria monocytogenes* infection in the mouse spleen. *J. Med. Microbiol.* 1996. **44**: 295–302.

27 Muraille, E., Giannino, R., Guirnalda, P., Leiner, I., Jung, S., Pamer, E. G. and Lauvau, G., Distinct in vivo dendritic cell activation by live versus killed *Listeria monocytogenes*. *Eur. J. Immunol.* 2005. **35**: 1463–1471.

28 Neuenhahn, M., Kerksiek, K. M., Nauerth, M., Suhre, M. H., Schiemann, M., Gebhardt, F. E., Stemberger, C. *et al.*, CD8alpha+dendritic cells are required for efficient entry of *Listeria monocytogenes* into the spleen. *Immunity* 2006. **25**: 619–630.

29 Dijkstra, C. D., Van Vliet, E., Dopp, E. A., van der Lelij, A. A. and Kraal, G., Marginal zone macrophages identified by a monoclonal antibody: characterization of immuno- and enzyme-histochemical properties and functional capacities. *Immunology* 1985. **55**: 23–30.

30 Metlay, J. P., Witmer-Pack, M. D., Agger, R., Crowley, M. T., Lawless, D. and Steinman, R. M., The distinct leukocyte integrins of mouse spleen dendritic cells as identified with new hamster monoclonal antibodies. *J. Exp. Med.* 1990. **171**: 1753–1771.

31 Mitchell, J., Lymphocyte circulation in the spleen. Marginal zone bridging channels and their possible role in cell traffic. *Immunology* 1973. **24**: 93–107.

32 Steinman, R. M., Pack, M. and Inaba, K., Dendritic cells in the T-cell areas of lymphoid organs. *Immunol. Rev.* 1997. **156**: 25–37.

33 Manders, E. M. M., Verbeek, F. J. and Aten, J. A., Measurement of colocalization of objects in dual-color confocal images. *J. Microsc.-Oxford* 1993. **169**: 375–382.

34 O'Riordan, M., Moors, M. A. and Portnoy, D. A., Listeria intracellular growth and virulence require host-derived lipoic acid. *Science* 2003. **302**: 462–464.

35 Aoshi, T., Zinselmeyer, B. H., Konjufca, V., Lynch, J. N., Zhang, X., Koide, Y. and Miller, M. J., Bacterial entry to the splenic white pulp initiates antigen presentation to CD8+T cells. *Immunity* 2008. **29**: 476–486.

36 Taylor, P. R., Martinez-Pomares, L., Stacey, M., Lin, H. H., Brown, G. D. and Gordon, S., Macrophage receptors and immune recognition. *Annu. Rev. Immunol.* 2005. **23**: 901–944.

37 Nussenzweig, M. C., Steinman, R. M., Witmer, M. D. and Gutchinov, B., A monoclonal antibody specific for mouse dendritic cells. *Proc. Natl. Acad. Sci. USA* 1982. **79**: 161–165.

38 Serbina, N. V., Salazar-Mather, T. P., Biron, C. A., Kuziel, W. A. and Pamer, E. G., TNF/iNOS-producing dendritic cells mediate innate immune defense against bacterial infection. *Immunity* 2003. **19**: 59–70.

39 Tam, M. A. and Wick, M. J., Differential expansion, activation and effector functions of conventional and plasmacytoid dendritic cells in mouse tissues transiently infected with *Listeria monocytogenes*. *Cell. Microbiol.* 2006. **8**: 1172–1187.

40 Arredouani, M., Yang, Z., Ning, Y., Qin, G., Soininen, R., Tryggvason, K. and Kobzik, L., The scavenger receptor MARCO is required for lung defense against pneumococcal pneumonia and inhaled particles. *J. Exp. Med.* 2004. **200**: 267–272.

41 Odermatt, B., Eppler, M., Leist, T. P., Hengartner, H. and Zinkernagel, R. M., Virus-triggered acquired immunodeficiency by cytotoxic T-cell-dependent destruction of antigen-presenting cells and lymph follicle structure. *Proc. Natl. Acad. Sci. USA* 1991. 88: 8252–8256.

42 Seiler, P., Aichele, P., Odermatt, B., Hengartner, H., Zinkernagel, R. M. and Schwendener, R. A., Crucial role of marginal zone macrophages and marginal zone metallophils in the clearance of lymphocytic choriomeningitis virus infection. *Eur. J. Immunol.* 1997. 27: 2626–2633.

43 Carrero, J. A., Calderon, B. and Unanue, E. R., Lymphocytes are detrimental during the early innate immune response against *Listeria monocytogenes*. *J. Exp. Med.* 2006. 203: 933–940.

Abbreviations: **LM:** *Listeria monocytogenes* · **MARCO:** macrophage receptor with collagenous structure · **MMM:** metallophilic marginal zone macrophage · **MZ:** marginal zone · **MZM:** marginal zone macrophage · **PALS:** periarteriolar lymphoid sheath · **pDC:** plasmacytoid DC · **RP:** red pulp

Full correspondence: Dr. Mark J. Miller, Department of Pathology and Immunology, Washington University School of Medicine, St. Louis, MO 63110, USA
Fax: +1-314-362-4096
e-mail: miller@pathology.wustl.edu

Additional correspondence: Dr. Emil R. Unanue, Department of Pathology and Immunology, Washington University School of Medicine, St. Louis, MO 63110, USA.
e-mail: unanue@wustl.edu

Supporting Information for this article is available at www.wiley-vch.de/contents/jc_2040/2009/38718_s.pdf

Received: 16/7/2008
Revised: 15/10/2008
Accepted: 19/11/2008